Journal of Applied Geophysics 119 (2015) 170–177

Contents lists available at ScienceDirect

Journal of Applied Geophysics

journal homepage: www.elsevier.com/locate/jappgeo

Examining lake-bottom structures with the resistivity imaging method in Ilan's Da-Hu Lake in Northeastern Taiwan

Ping-Yu Chang [a,*], Liang-Chi Chang [a], Teh-Quei Lee [b], Yu-Chang Chan [b], Huei-Fen Chen [c]

[a] Dept. of Geosciences, National Central University, Jhong-li, Taiwan
[b] Institute of Earth Sciences, Academia Sinica, Taipei, Taiwan
[c] Inst. of Applied Geosciences, National Taiwan Ocean University, Keelung, Taiwan

ARTICLE INFO

Article history:
Received 6 January 2015
Received in revised form 23 April 2015
Accepted 21 May 2015
Available online 27 May 2015

Keywords:
Electrical resistivity method
Floating electrodes
Da-Hu Lake
Water-borne
Lake-bottom structures

ABSTRACT

In this study, we used the electrical resistivity method for imaging subsurface structures of lake-bottom sediment in Da-Hu Lake in Ilan, Taiwan. Floating passive electrodes were used for the surveys in the study area. We deployed eighteen survey lines across the lake, and executed the survey with the Schlumberger and Wenner array. There are two geological cores, DH-7A and DH-7B, located at different locations in Da-Hu Lake. The cores were carefully collected for the purpose of the sediment and dating analyses, as well as for the geochemical testing, which can be useful to climate-change studies covering the past 10,000 years. The inverted images clarify the spatial relationships between the sediment and basement structures. The sediments above the resistive rock basement consisted of the sand sediments (from 45 to 60 Ω m) and mud sediments (less than 30 Ω m). The results of our study show that a sandy layer comprising slate debris with a resistivity of 45 to 60 Ω m is located 3 to 8 m under the water's surface in the eastern part of the lake, and the outcomes confirm the findings from the DH-7A core data. The resistivity spatial distribution suggests that the lake's sand layer originally came from a region east of the lake. We also found a sharp linear resistivity structure in the western part of the lake. The structure's strike is consistent with observations from the normal fault's surface outcrops near the western part of the lake. Consequently, we infer that this structure line might be a stretch of the normal fault and that the two cores are located at the hanging wall as well. In addition, the results show that we can use the electrical resistivity imaging method with floating passive electrodes to investigate the lake-bottom in detail.

1. Introduction

In the study we attempt to use resistivity imaging method with floating electrodes to investigate the sub-bottom sedimentary structures in Taiwan's Da-Hu Lake. The lake is one of the fringe lakes located between the Ilan Plain and the mountain range surrounding the plain (Fig. 1). Between the plain and the surrounding mountain range, there are a few lakes located on the subsided hanging wall of the rifting normal fault systems. Because some of these lakes are far away from the main Lanyangchi River system, only huge flooding events can bring massive amounts of coarse sediment into these lakes. Hence, we believe that sub-bottom sedimentary structures may contain preserved records of climate changes during the past 10,000 years. Borehole investigations and geophysical surveys are frequently used for reconstructing the sedimentary history and the sediment geometries. However, the average water depths of these fringe lakes are below 1 to 2 m and made it difficult to conduct the ordinary water-borne geophysical surveys, such as sub-bottom profilers. Hence we have collected core samples and conducted surface resistivity surveys across the lake in order to construct the spatial geometries of the sediments under the lake's bottom. We have shown that the resistivity imaging surveys with floating electrodes provide sufficient resolution for the requirements of the climate-change research in Da-Hu Lake. In combination with the core records, we can shed light on the possible sources of—and event explanations for—the lake deposits.

2. Geological settings

The Ilan Plain is thought to have taken shape from the extension of the Okinawa Trough back arc basin within the Eurasian continental lithosphere (Lai et al., 2009). The recent extension of the Okinawa Trough by approximately 0.1 Ma involved ENE- and WSW-trending normal faults dipping toward the Okinawa Trough axis with offsets from a few meters to tens of meters (Lai et al., 2009; Sibuet et al., 1998) in the westernmost part of the trough. Unconsolidated alluvial deposits from the Lanyangchi River were laid over the rock basement exhibiting the normal faults (Chiang et al., 1979; Hsu et al., 1996) from seismic reflection and refraction profiles. According to the drilling core records, young sediment deposited on the plain at an extremely high deposition rate, exceeding a 20-m thickness within the last 3000 years and a 120-m

* Corresponding author.
E-mail address: pingyuc@ncu.edu.tw (C. Ping-Yu).

http://dx.doi.org/10.1016/j.jappgeo.2015.05.016
0926-9851/

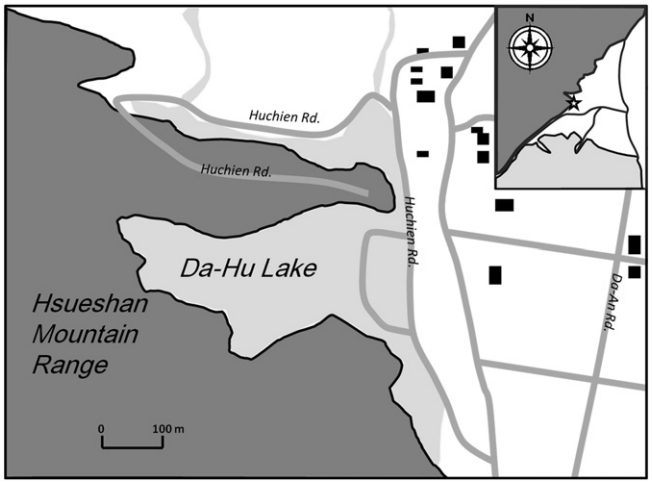

Fig. 1. An area map of Da-Hu Lake in northeastern Taiwan's Ilan region.

thickness in Holocene (CGS, 2001; Chen, 2000). The findings suggest that the plain underwent a rapid subsidence recently.

We collected core samples from two boreholes, DH-7A And DH-7B in the lake (Fig. 2a) for our studies on the climate change in the Ilan Plain. In addition, we conducted electrical resistivity surveys in Da-Hu Lake to correlate the distribution of sediment found in the core samples. The western and southern sections of Da-Hu Lake are bounded by the Hsuehshan Mountain Range. The Eocene Chungling Formation outcrops on the western side of Da-Hu Lake, and the Chungling Formation is overlain by the Hsitsun Formation, which can be observed on the southern side of the lake. The two formations consist of intercalated quartz sandstone and slate (Ooe, 1931). As noted, two geological boreholes, DH-7A and DH-7B, were completed in the lake (Wen, 2011). The core logs show that the lake bottom consisted of mainly Holocene sediment with a thickness of over 20 m (Fig. 2b). The core logs of DH-7B indicate that the borehole reaches the slate basement at a depth of 35 m below the lake bottom. The C-14 dating shows that the sediment above the slate basement was deposited within the last 7500 years. Both the sediment in DH-7A and the sediment in DH-7B are mostly clay, with thin sand layers that are mostly less than 1-m thick. In DH-7B we observed a 2-m-thick sandy layer at about 6–8 m below the lake bottom. C-14 dating indicates that the top of this sandy layer was deposited about 1200 yrBP (years before present). On the other hand, we found a coarse sand layer at about 3–5 m, 6.5–7.5 m, and 10–11 m below the lake bottom in DH-7A; and the C-14 dating records show that the deposition time was earlier than 1700 yrBP for the 6.5–7.5 m sand layer in DH-7A. The inconsistencies in the core records of DH-7A and DH-7B raise significant questions about the spatial relationships among sand deposits in Da-Hu Lake. Fault movements or sedimentary events are two possible reasons for the inconsistent sand deposits. To further investigate the possible causes of the inconsistencies, we deployed several resistivity surveys in Da-Hu Lake: our specific aim was to resolve the spatial relationships between boreholes DH-7A and DH-7B.

3. Survey configurations

Researchers frequently use resistivity imaging methods in various environments to investigate subsurface structures (e.g., Binley et al., 2002; Chang et al., 2011; Kemna et al., 2002; Kim et al., 2002; Mitchell et al., 2008; L. Toran et al., 2010b; van Schoor, 2002). Loke et al. (2013) gave a good review of the developments of a variety of resistivity surveys. Among these studies, a few researchers used waterborne resistivity surveys for geological mapping (Rinaldi et al., 2006; Rucker et al., 2011) and submarine groundwater discharge (Day-Lewis et al., 2006; Henderson et al., 2010; Swarzenski et al., 2007). In the current study, we conducted resistivity imaging surveys with the Lippmann 4-point Light system and passive electrodes. Compared to the active electrodes which have built-in addressed electronics on each one, these passive electrodes are consisted in copper conductors connected with a cable. We used a multiplexer to transmit relay information and measurements to and from the passive electrodes. We used the Wenner–Schlumberger array to improve the signal-to-noise ratio, as well as a floating electrode cable to collect measurements. Loke and Lane (2004) compared measurements based on floating electrode arrays to measurements based on bottom arrays in simulation studies, and concluded that the inversion should include water-column thickness and resistivity to avoid artifacts and that in the case of floating arrays, water depth should be no more than 25% of the depth of investigation. For consideration of water depths, Toran et al. (2010a) selected both a floating cable and bottom systems for electrical surveys of Mirror Lake. Because the maximum depth of Da-Hu Lake is less than 2.5 m and the wanted exploration depth is about 30 m, we chose a maximum length of 100 m for the current electrode spacing with the electrode spacing kept at 1 m to acquire higher-resolution measurements. Water depths under the survey lines were measured with a weighted sounding line for the inversion purposes. To cover as large an area as possible in an efficient way, we moved the passive cable in a fan-like geometrical pattern while one end of the electrode cable was stationed at a fixed location (Fig. 2a). The resistivity meter and the multiplexer were stationed on the shore, and the tail end of the passive cable was tightly secured to a rod pinned down to the lake bottom. After completing one measurement, a boat then towed the floating cable and the cable end to a new measuring position and pinned the end for the next measurement. We have completed 18 resistivity survey lines in Da-Hu Lake. The measured resistivity data were then inverted with EarthImager 2D™ code (AGI, 2009). The average inversion RMS error was about 13.7%. RMS errors higher than 15% were found only in the three survey lines in the southern part of the lake. The three measurements had an average RMS error of 31.0%. Zhou and Dahlin (2003) concluded that a 10% error for the in-line electrode spacing will result in a similar estimation error on the inverted resistivity for the Schlumberger arrays. Because the surveys with high RMS errors were all completed under windy conditions, we concluded that the errors had arisen owing to the drifting of floating cables and electrodes in these conditions.

4. Results

We have conducted water-borne surveys with a resistivity meter placed on the northern, western, southern, and eastern shores while the end of the electrode cable was moved in Da-Hu Lake. Borehole DH-7A was located within the surveys' coverage area on the lake's northern side. Fig. 3(a) through (d) shows the inverted resistivity profiles, including lines 4, 5, 6, and 7, located on the northern side of the lake. Because we had placed the resistivity meter on shore, the first electrode (position marked at 0 m) placed in the water was about 2 m near the shoreline and the rest of the electrodes were deployed further into the center of the lake. An outcrop of slate can be observed at the location where we placed the resistivity meter. Hence the first few electrodes should provide direct responses to the slate basement of Da-Hu Lake. Among the survey lines, line 4 was the one nearest the slate shoreline; therefore, we expected it would exhibit significant responses to the slate basement. In the inverted images, we observed that a resistive basement with resistivity over 75 Ω m was located near the shoreline, and that the depth of the basement increased quickly from the lakeshore into the lake center. The depth of the resistive basement was over 20-m deep in the center of the lake. The topography of the resistive basement implies that the top surface of the slate basement exceeded a depth of 20 m in the center of the lake. In addition to the very resistive basement, the surface of the lake deposits comprised a resistive layer with resistivity between 45 and 60 Ω m. The thickness of the layer was between 5 and 7 m. Below the resistive sediments was a conductive layer with resistivity less than 30 Ω m. The conductive layer lay on top of the resistive basement and its thickness appeared to exceed 12 m.

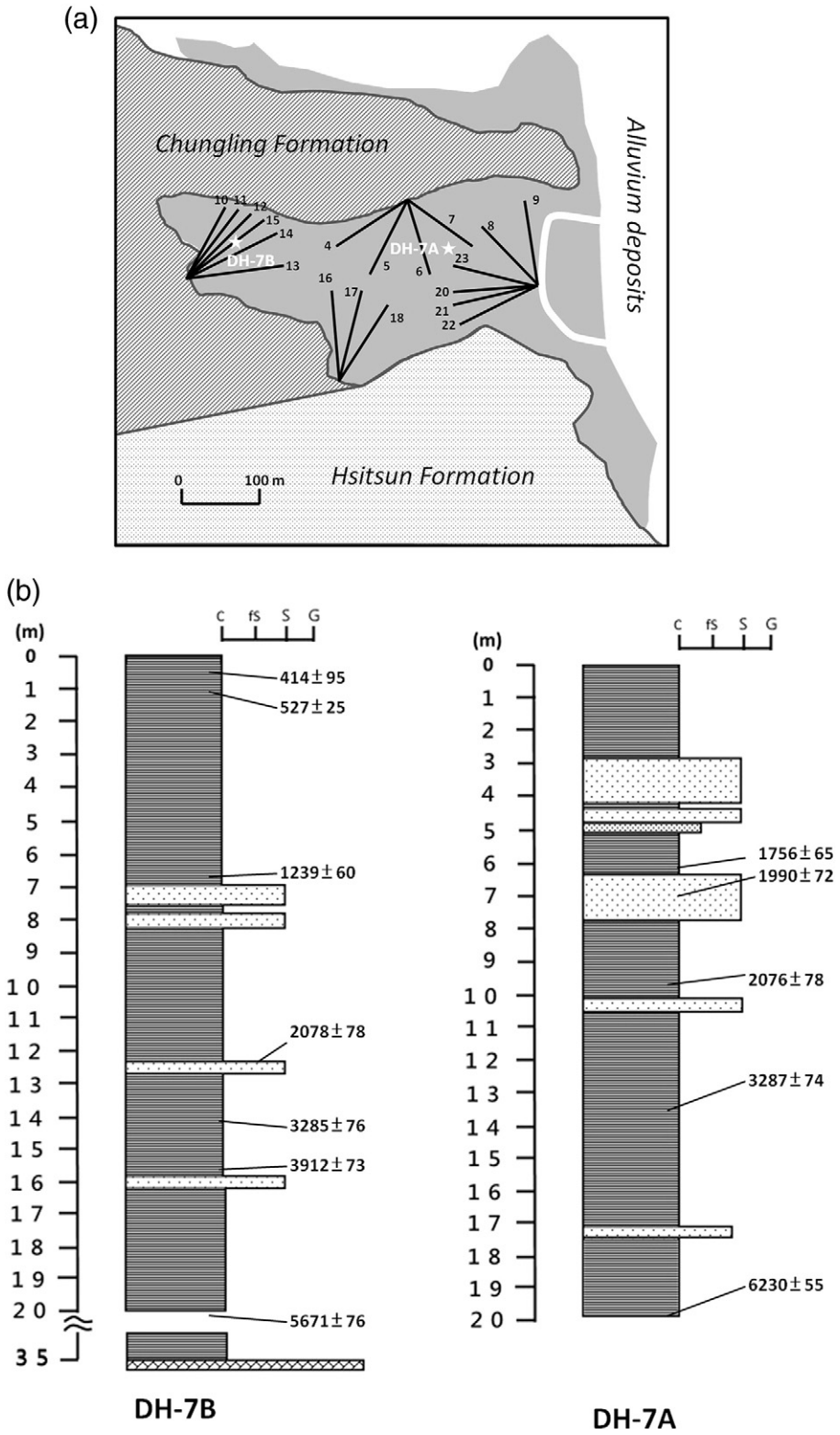

Fig. 2. (a) Locations of boreholes DH-7A and DH-7B and the resistivity survey lines in Da-Hu Lake, (b) core records of DH-7A and DH-7B (numbers show the C-14 dating value).

The borehole DH-7A was located between line 6 and line 7. Compared with the core records of the DH-7A (Fig. 4a), the surface resistive layer with resistivity between 45 and 60 Ω m probably consisted of debris layers found about 3 to 8 m below the lake's bottom; and the conductive layer consisted of mud sediments about 8 to 20 m below the lake's bottom.

Fig. 5 presents the images of lines 10, 11, 12, 15, 13, and 14 in the western part of Da-Hu Lake. Lines 10 and 11 were close to the shore consisting of slates, and hence, we found that a resistive structure was located at the basement of the profile and that the top of the resistive structure's surface varied from about 5 m to 10 m below the lake's surface. The lake's other borehole, DH-7B, was located between line 15 and

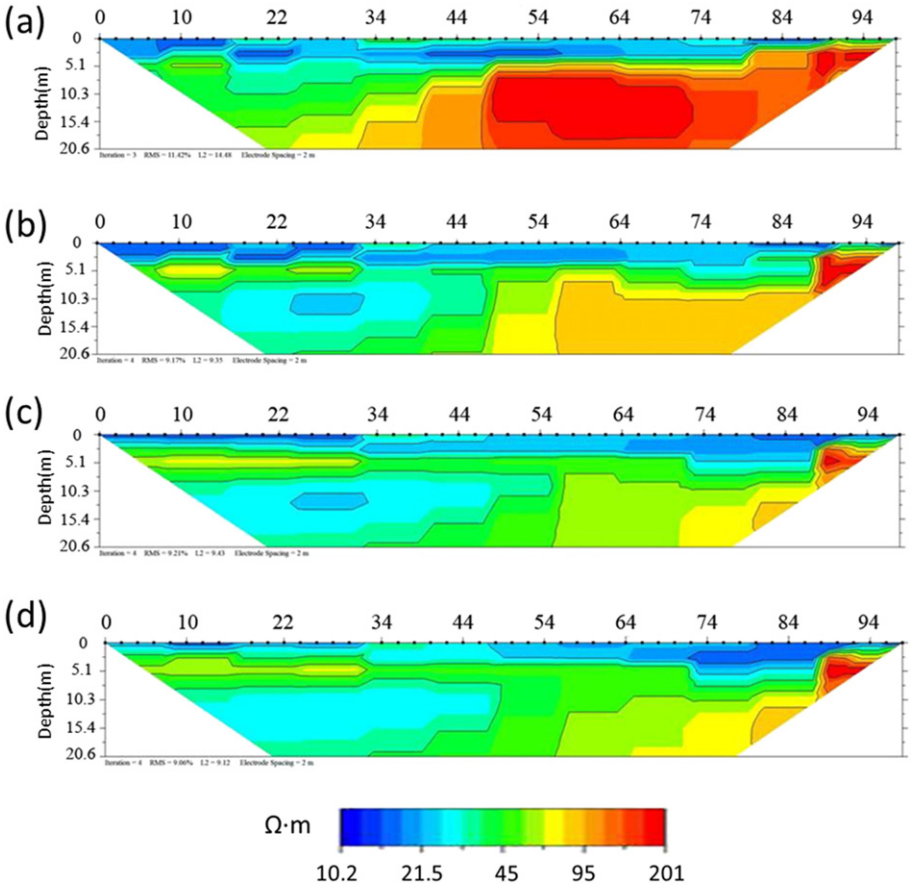

Fig. 3. The inverted resistivity profiles of (a) line 4, (b) line 5, (c) line 6, and (d) line 7 on the northern side of Da-Hu Lake. (The "0 distance mark" is the location of the resistivity meter on shore.)

line 14. Both lines 15 and 14 revealed that a resistive structure was located at the beginning of the lines, and that this resistive structure's surface descended into the lake from near the lake's surface to more than 18 m below the lake's surface. The resistive structure may have been the lake's slate basement and the structure's depth increased rapidly in the western part of the lake. We also found the same resistivity structure in the inverted image of line 13. In the profiles of lines 13, 14, and 15, conductive sediment with resistivity less than 30 Ω m was the major material covering the slate basement. Sporadic lenses of resistive deposits, with resistivity between 45 and 60 Ω m, can be observed 3 to 7 m below the lake's surface. After comparing the resistivity images with the core records from DH-7B (Fig. 4b), we concluded that the basement was located at a depth over 20 m in the center of the lake, and that the conductive deposits consisted of conductive mud materials with sporadic sand lenses, which are relatively resistive to the clay-like mud deposits.

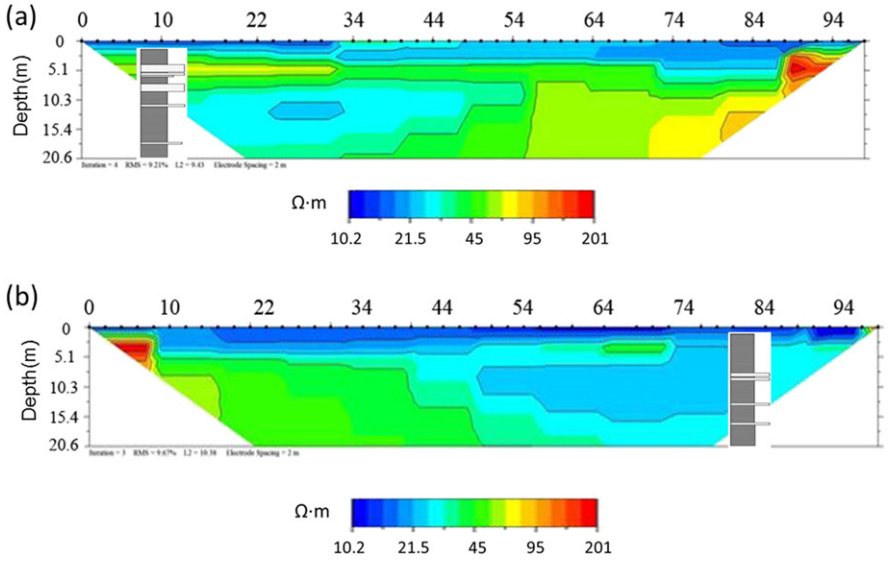

Fig. 4. A comparison of core records with the resistivity images for (a) DH-7A and an inverted profile of line 6, and (b) DH-7B and an inverted profile of line 14.

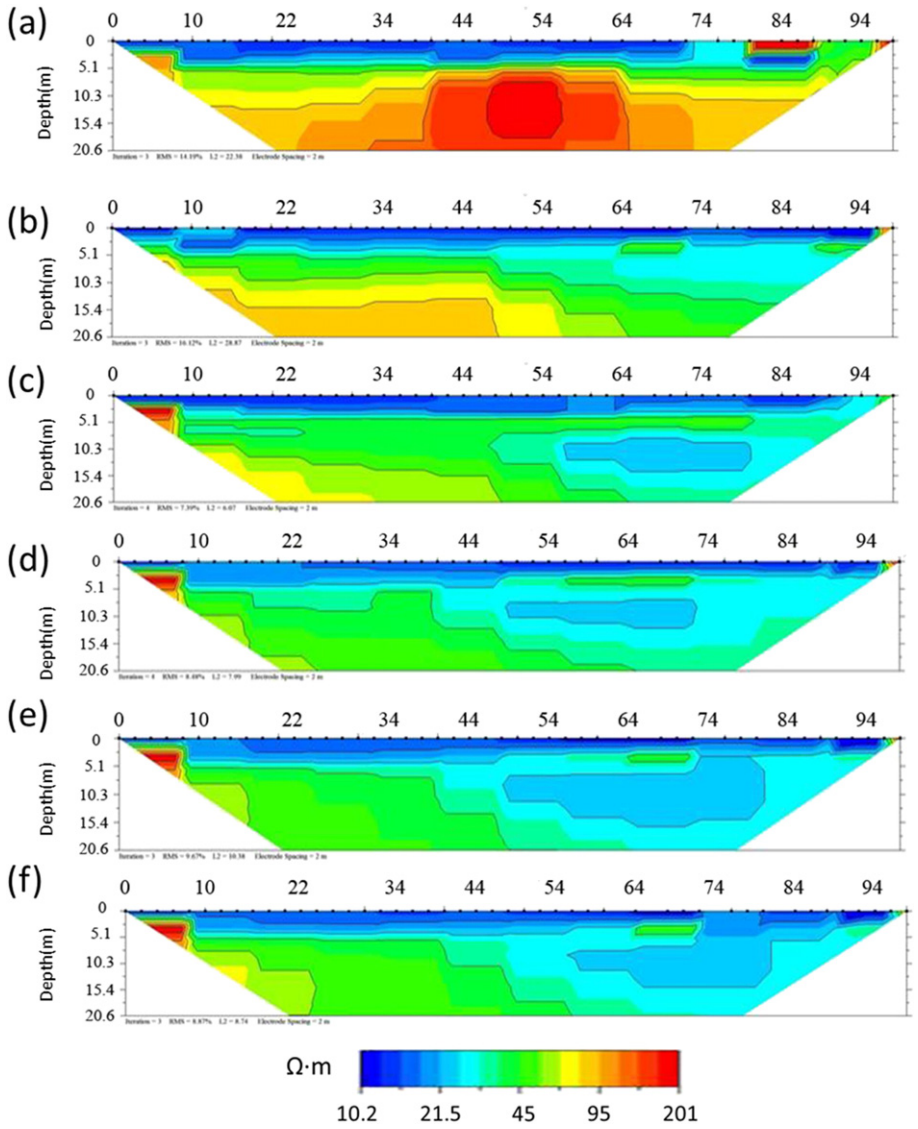

Fig. 5. The inverted resistivity profiles of (a) line 10, (b) line 11, (c) line 12, (d) line 15, (e) line 14, and (f) line 13 on the western side of Da-Hu Lake. (The "0 distance mark" is the location of the resistivity meter on shore.)

Fig. 6 shows the inverted resistivity images of lines 9, 8, 23, 21, and 22 in a counterclockwise order in the eastern part of Da-Hu Lake. The aforementioned borehole DH-7A was located near lines 8 and 23. The maximum exploration depths of the inverted images were between 17 and 20 m. Similar to the images from the northern part of the lake, the images from the eastern part reveal that a layer of sediment with resistivity between 45 and 60 Ω m was between 5 and 10 m below the lake's surface. We have observed that sediment below this layer had resistivity less than 30 Ω m. When we compared resistivity images in Fig. 6 with core records of DH-7A, we found that the sediment layer with resistivity between 45 and 60 Ω m corresponded to the debris layer between 3 and 8 m below the lake's bottom (i.e., 5–10 m below the lake's surface). The relatively conductive sediment below this layer was the clay-like deposits. Line 22 is the line closest to the southern lake shore. The inverted images of line 22 show that the descending slate basement had a resistivity higher than 100 Ω m. The top of the slate basement descended into the lake from near the surface to a depth more than 20 m.

Fig. 7 presents the inverted resistivity images from the survey lines 16, 17, and 18 at the southern part of the lake. In general, the sediment that was between 3 and 7 m below the lake's surface consisted of very resistive materials in all southern lines. The resistivity of the sediment was greater than 100 Ω m and rose the closer one got to shore. Away from the shoreline we observed a relatively conductive layer with resistivity less than 30 Ω m located below the resistive layer. The thickness of the conductive layer was possibly more than 15 m in the center of the lake. The resistive layer probably corresponded to the debris layer found in DH-7A, and the lower conductive layer was likely made up of mud deposits.

5. Discussion

The core records and C-14 dating results from boreholes DH-7A and DH-7B show that the two cores had a similar deposition rate of about 2.59 and 2.96 mm/yr, respectively, for the muddy deposits (dating from about 6000 to 3000 yrBP) that were 20 m to 15 m under the lake's surface (Fig. 8). The deposition rate suddenly rose in both DH-7A and DH-7B sometime after approximately 2000 yrBP. The average deposition rate had reached 10.13 mm/yr in DH-7A and 7.26 mm/yr in DH-7B soon after 2200 yrBP. The deposition rate returned to an average of about 2.98 mm/yr after 2000 yrBP in DH-7A, yet the rate remained at an average of about 7 mm/yr until about 600 yrBP in DH-7B. DH-7B had a deposition rate of about 2.75 mm/yr after 600 yrBP. In addition, we have also noticed that the portion of sand sediment consisting of

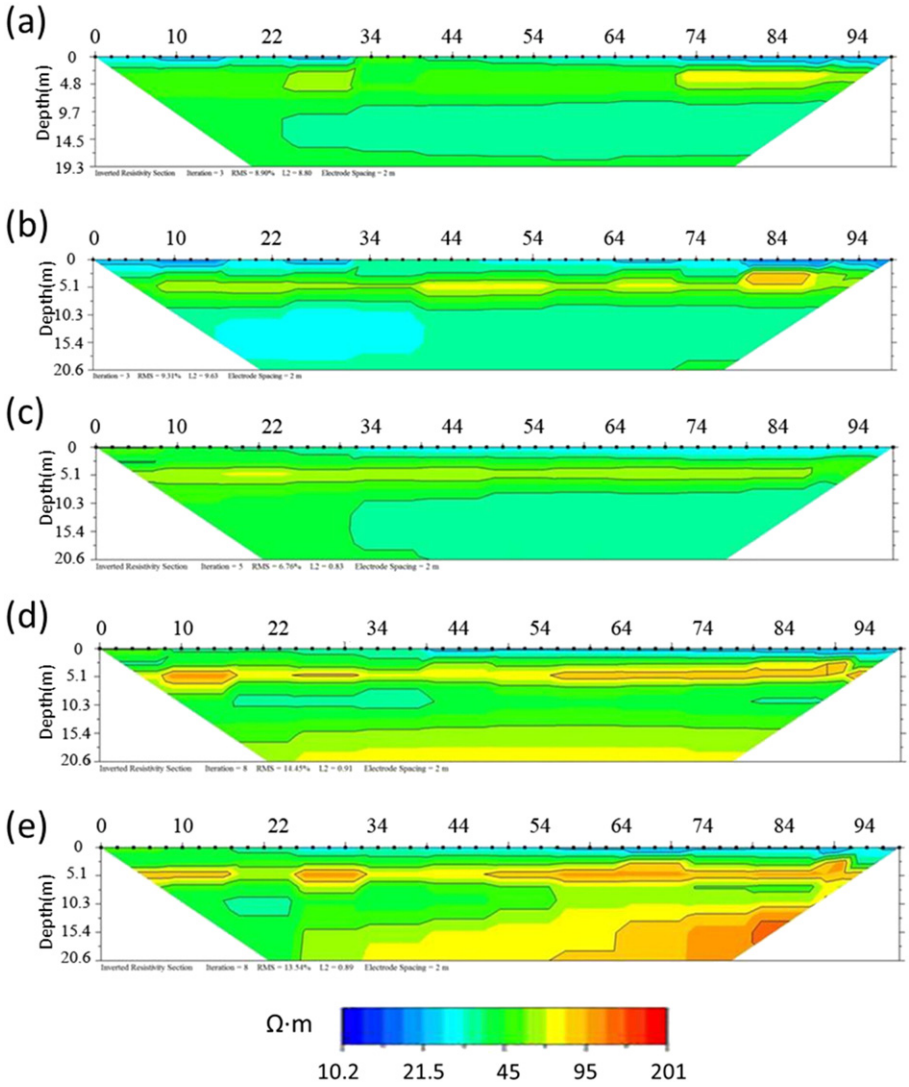

Fig. 6. The inverted resistivity profiles of (a) line 16, (b) line 17, and (c) line 18 on the southern side of Da-Hu Lake. (The "0 distance mark" is the location of the resistivity meter on shore.)

slate debris increased after 2000 yrBP at a location approximately 5 m to 9 m below the lake's surface. In addition, this same slate-debris sediment is absent in DH-7B. Hence, researchers should clarify the spatial distribution of sediment at different depths in order to identify the evolutionary mechanisms and history of Da-Hu Lake.

Fig. 9 shows the maps of resistivity at different depths below the lake's surface. We constructed the resistivity maps by interpolating the inverted resistivity results from all survey lines in Da-Hu Lake. The map at −5 m shows that the southeastern part of the lake was filled with resistive sediment (resistivity higher than 50 Ω m), which can be correlated to the slate-debris layer indicated in the DH-7A core records. The eastern part of the lake was still covered with resistive sediment of slate debris whose resistivity was higher than 45 Ω m at −8 m. This resistive slate debris, however, did not cover the western part of the lake at the same depths. The finding explains why we did not find the same debris layer in DH-7B. It seems that the debris had been coming from the southeastern hills, and had washed into Da-Hu Lake because the debris sediment gradually pinched out from the southeastern area to the center of the lake. According to the C-14 dating, the debris-flow event may have happened sometime after 2000 yrBP. The western part of the lake, on the other hand, had lacked thick layers of slate debris since 6000 yrBP, because the resistivity map shows that the resistive debris layer was, at the time of our observations, located only in the eastern part of the lake throughout different depths. The findings imply that the eastern part of the lake was filled with coarse sediment from the southwest while the western part of the lake had remained the same depositional environment after 2000 yrBP.

The debris-flow event may explain the deposition-rate difference between DH-7A and DH-7B after 2000 yrBP, yet we still need to further examine the possible reasons for such a sudden change of the deposition rate in the two borehole records at about 2000 yrBP. As shown in Fig. 9, we found that the resistivity near DH-7A and DH-7B was dipping below 25 Ω m at a location approximately 10 m to 13 m below the lake's surface. This depth range is correlated to the periods when a sudden change of deposition rates took place, as revealed in the core records. We conclude that the sediment with low resistivity consists of clay-mineral deposits. Several factors can increase clay minerals and accelerate deposition rates of lake deposits. Among these factors, humidity and tectonic/structural movements may be the most likely mechanisms for the sudden change of Da-Hu Lake's sedimentary deposition rate about 2200 yrBP. According to Lin et al. (2004), the Ilan area has undergone periods of significant increase of humidity between about 3200 and 3100 yrBP, 2000 to 1300 yrBP, and after 900 yrBP, and the evidence for this conclusion rests on pollen records of the Wuyuan core in Ilan. In short, humidity appears to be the chief reason for the accelerated deposition rate between 2000 and 600 yrBP in Da-Hu Lake.

If the sedimentary basin has a fairly constant space and a growing deposition rate, the basin will soon fill up with detrital sediment.

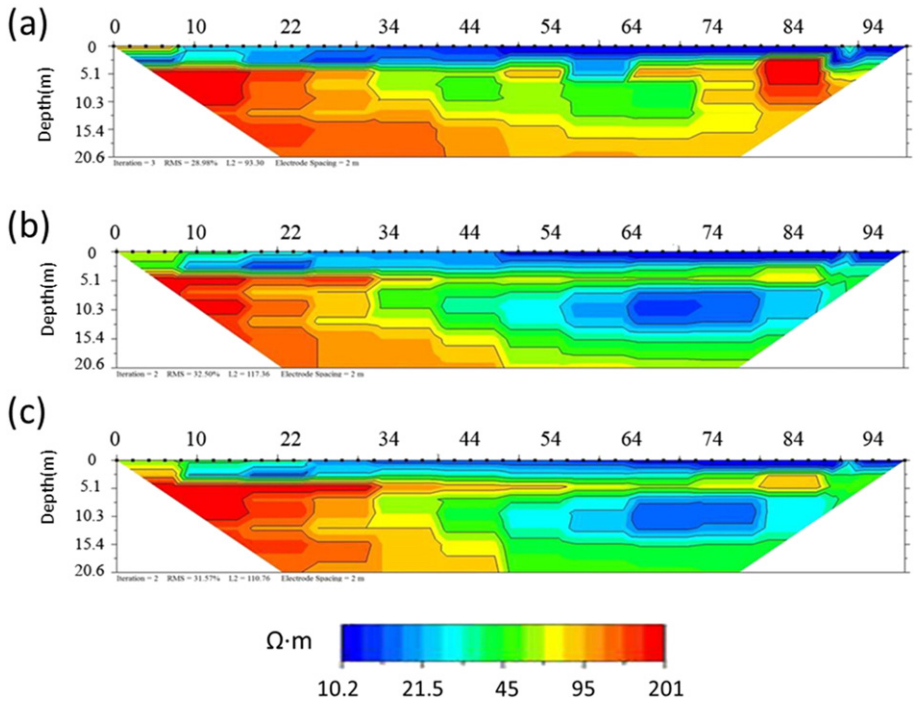

Fig. 7. The inverted resistivity profiles of (a) line 9, (b) line 8, (c) line 23, (d) line 21, and (e) line 22 on the eastern side of Da-Hu Lake. (The "0 distance mark" is the location of the resistivity meter on shore.)

Therefore, tectonic subsidence may be another factor responsible for the rapid deposition rate. In addition to the low-resistivity sediment, we observed quite clearly a linear structure appearing in the northwestern part of the lake at −13 m (see Fig. 9). The lineage was likely a fault structure where the line of strike passed through the northwestern side of DH-7B. LiDAR images of the surrounding area and the field survey show that a normal fault lay on the southeastern hillside in the extended direction of this fault line. Boreholes DH-7A and DH-7B—and most of Da-Hu Lake—were on the hanging wall of the fault. One of the possible reasons for the sudden change of Da-Hu Lake's sedimentary deposition rate about 2200 yrBP is that the fault had been active from 2200 to 600 yrBP. The downward movement of the hanging wall may have caused the quick subsidence of the lake's bedrock and subsequent rapid accumulation of mud sediment. It seems that the sedimentation rates in DH-7A and DH-7B returned to about 2.7–2.9 mm/yr after 600 yrBP; and this finding implies that the active faulting movement has come to an end and that the lake has, thus, returned to its "normal" environment, which had prevailed before 2000 yrBP.

Our resistivity data and core-analysis results have shaped our understanding of Da-Hu Lake's evolution over the past 6000 years. From 6000 to about 2200 yrBP, Da-Hu Lake remained a stable environment and constantly received fine detrital sediment from nearby hills. Yet at about 2000 yrBP, the lake's active subsidence and the humid climate resulted in the sudden change of the deposition rate. Later, about 1700 yrBP, sediment consisting of slate debris from the southwest filled in the eastern part of the lake. The shallower topography of eastern Da-Hu Lake resulted in reduced sediment buildup between 1700 yrBP and 600 yrBP, while rapid deposition continued to characterize the western part of the lake. After 600 yrBP the entire lake was again in an environment similar to that before 2000 yrBP and the deposition rate slowed to about 2.7 mm/yr.

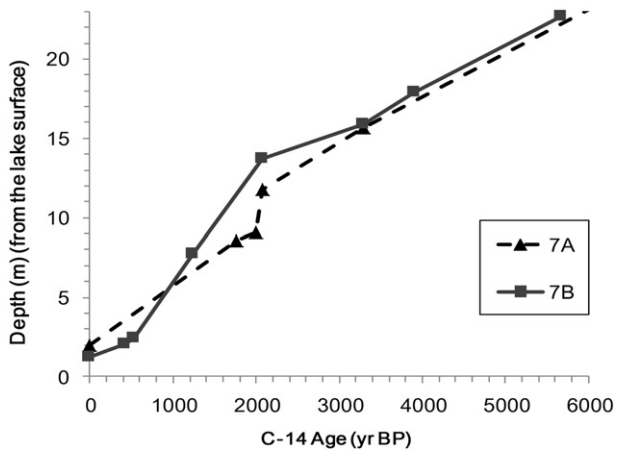

Fig. 8. The relationships between the C-14 dated age and the depths for deposits in boreholes DH-7A and DH-7B.

6. Conclusions

We used the electrical resistivity method to image subsurface structures of Da-Hu Lake's bottom sediment in Ilan, Taiwan. We used floating passive electrodes for the surveys in the study area and deployed 24 survey lines across the lake. Compared to the core logs from two geological cores, DH-7A and DH-7B, the inverted resistivity images greatly clarify the spatial relationships between the sediment and the basement structures of the lake. In general, the resistivity images are consistent with the core records from DH-7A and DH-7B. The sediment above the resistive rock basement consisted chiefly of mud with resistivity from 20 to 25 Ω m as shown in the records in DH-7B. In DH-7A, a sandy layer consisting of slate debris exhibited a higher-resistivity structure (45 to 60 Ω m) located between 3 m and 8 m under the water's surface in the eastern part of the lake. The spatial distribution of the slate debris suggests that this layer possibly came from an area southeast of the lake; and the C-14 dating shows that the layer emerged in the lake sometime after 2000 yrBP. In addition, we observed evidence of a linear resistivity structure in the western part of the lake. Its strike was consistent with our observations from the surface outcrops of the normal fault near the western part of the lake. We infer that this structure line might

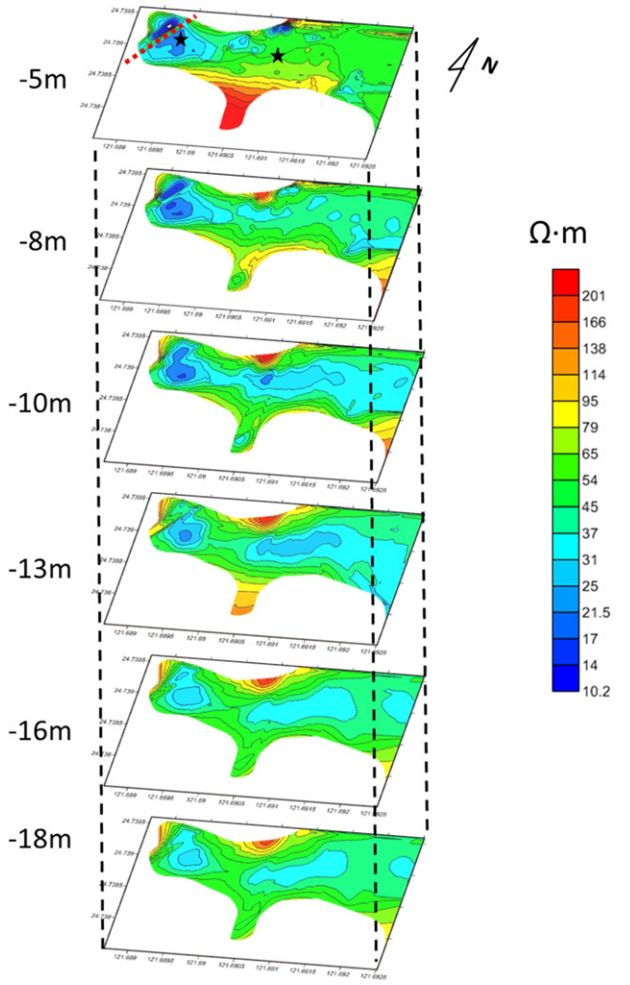

Fig. 9. The interpolated resistivity maps of different depths relative to the surface of Da-Hu Lake. The stars and the dotted line show the locations of the boreholes and the inferred fault, respectively.

be a stretch of the normal fault. The two cores and most of Da-Hu Lake are located at the hanging wall. The subsidence of the hanging wall resulted in the formation of the lake. In conclusion, the results show that we can use the electrical-resistivity imaging method with floating passive electrodes to investigate lake bottoms in detail.

Acknowledgment

This study is funded by the Ministry of Science and Technology, Taiwan under the project grant NSC98-3114-M-002-001.

References

AGI, 2009. Instruction Manual for EarthImager 2D Version 2.4.0, Edited. Advanced Geosciences, Inc., Austin, Texas.

Binley, A., Cassiani, G., Middleton, R., Winship, P., 2002. Vadose zone flow model parameterisation using cross-borehole radar and resistivity imaging. J. Hydrol. 267 (3), 147–159.

CGS, 2001. Groundwater Monitoring Network in Taiwan: The Hydro-geology Survey in the Chianan Plain and Lanyang Plain*Rep*. Central Geological Survey, Taipei (212 pp. pp).

Chang, P.-Y., Chang, S.-K., Liu, H.-C., Wang, S.C., 2011. Using integrated 2D and 3D resistivity imaging methods for illustrating the mud-fluid conduits of the Wushanting Mud Volcanoes in Southwestern Taiwan. Terr. Atmos. Ocean. Sci. 22 (1), 1–14.

Chen, W.-S., 2000. Sedimentary environment analysis and stratigraphic correlations–Lanyang Plain (in Chinese), Cent. Geol. Surv. Rep (89-17, 49 pp., Cent. Geol. Surv., Ministry Econ. Affairs, Taipei, Taiwan).

Chiang, S.C., Lin, J.J., Chang, C.R.Y., Wu, T.M., 1979. A preliminary study of the Chingshui geothermal area, Ilan, Taiwan. Proceedings Fifth Geothermal Workshop. Geothermal Reservoir Engineering, Stanford, USA, pp. 249–254.

Day-Lewis, F.D., White, E.A., Johnson, C.D., Lane, J.W., Belaval, M., 2006. Continuous resistivity profiling to delineate submarine groundwater discharge — examples and limitations. Lead. Edge (Tulsa, OK) 25 (6), 724–728.

Henderson, R.D., Day-Lewis, F.D., Abarca, E., Harvey, C.F., Karam, H.N., Liu, L., Lane Jr., J.W., 2010. Marine electrical resistivity imaging of submarine groundwater discharge: sensitivity analysis and application in Waquoit Bay, Massachusetts, USA. Hydrogeol. J. 18 (1), 173–185.

Hsu, S.K., Sibuet, J.C., Shyu, C.T., 1996. High-resolution detection of geologic boundaries from potential-field anomalies; an enhanced analytic signal technique. Geophysics 61 (2), 373.

Kemna, A., Kulessa, B., Vereecken, H., 2002. Imaging and characterisation of subsurface solute transport using electrical resistivity tomography (ERT) and equivalent transport models. J. Hydrol. 267 (3), 125–146.

Kim, J.-H., Yi, M.-J., Song, Y., Cho, S.-J., Chung, S.-H., Kim, K.-S., 2002. DC resistivity survey to image faults beneath a riverbed. paper presented at 15th EEGS Symposium on the Application of Geophysics to Engineering and Environmental Problems.

Lai, K.Y., Chen, Y.G., Wu, Y.M., Avouac, J.P., Kuo, Y.T., Wang, Y., Chang, C.H., Lin, K.C., 2009. The 2005 Ilan earthquake doublet and seismic crisis in northeastern Taiwan: evidence for dyke intrusion associated with on-land propagation of the Okinawa Trough. Geophys. J. Int. 179 (2), 678–686.

Lin, S.-F., Liew, P.-M., Lai, T.-H., 2004. Late Holocene pollen sequence of the Ilan Plain, northeastern Taiwan, and its environmental and climatic implications. Atmos. Ocean. Sci. 15 (2), 221–237.

Loke, M.H., Lane, J.W.J., 2004. Inversion of data from electrical resistivity imaging surveys in water-covered areas. Explor. Geophys. 35, 266–271.

Loke, M.H., Chambers, J.E., Rucker, D.F., Kuras, O., Wilkinson, P.B., 2013. Recent developments in the direct-current geoelectrical imaging method. J. Appl. Geophys. 95 (0), 135–156. http://dx.doi.org/10.1016/j.jappgeo.2013.02.017.

Mitchell, N., Nyquist, J.E., Toran, L., Rosenberry, D.O., Mikochik, J.S., 2008. Electrical resistivity as a tool for identifying geologic heterogeneities which control seepage at Mirror Lake, Nh. paper presented at 21st EEGS Symposium on the Application of Geophysics to Engineering and Environmental Problems.

Ooe, J., 1931. In: B. o. P. Industries (Ed.), Explanatory Text of the Geological Map of Taiwan: Ritozan Sheet, p. 26.

Rinaldi, V., Guichon, M., Ferrero, V., Serrano, C., Ponti, N., 2006. Resistivity survey of the subsurface conditions in the estuary of the Rio de la Plata. J. Geotech. Geoenviron. 132 (1), 72–79.

Rucker, D.F., Noonan, G., Greenwood, W.J., 2011. Electrical resistivity in support of geological mapping along the Panama Canal. Eng. Geol. 117 (1–2), 121–133.

Sibuet, J.C., Deffontaines, B., Hsu, S., Thareau, N., 1998. Okinawa trough backarc basin: early tectonic and magmatic evolution. J. Geophys. Res. 103 (B12) (30245-30230,30267).

Swarzenski, P.W., Simonds, F.W., Paulson, A.J., Kruse, S., Reich, C., 2007. Geochemical and geophysical examination of submarine groundwater discharge and associated nutrient loading estimates into lynch cove, Hood Canal, WA. Environ. Sci. Technol. 41 (20), 7022–7029.

Toran, L., Johnson, M., Nyquist, J., Rosenberry, D., 2010a. Delineating a road-salt plume in lakebed sediments using electrical resistivity, piezometers, and seepage meters at Mirror Lake, New Hampshire, USA. Geophysics 75 (4), WA75–WA83.

Toran, L., Johnson, M., Nyquist, J., Rosenberry, D., 2010b. Delineating a road salt plume in lakebed sediments using electrical resistivity, piezometers, and seepage meters at Mirror Lake, NH. Geophysics 75 (4), 73–85.

van Schoor, M., 2002. Detection of sinkholes using 2D electrical resistivity imaging. J. Appl. Geophys. 50 (4), 393–399.

Wen, S.-Y., 2011. Environmental Changes in Ilan Region Since 8 Ka, Taiwan. National Taiwan Ocean University (102 pp.).

Zhou, B., Dahlin, T., 2003. Properties and effects of measurement errors on 2D resistivity imaging surveying. Near Surf. Geophys. 1 (3), 105–117.